Exploring a new interaction between dark matter and dark energy using the growth rate of structure

Martín G. Richarte*
Departamento de Física, Facultad de Ciencias Exactas y Naturales, Universidad de Buenos Aires and IFIBA, CONICET, Ciudad Universitaria 1428, Pabellón I, Buenos Aires, Argentina

Lixin Xu†
Institute of Theoretical Physics, School of Physics and Optoelectronic Technology, Dalian University of Technology, Dalian, 116024, People's Republic of China and State Key Laboratory of Theoretical Physics, Institute of Theoretical Physics, Chinese Academy of Sciences, Beijing 100190, People's Republic of China

(Dated: June 9, 2015)

We present a phenomenological interaction with a scale factor power law form which leads to the appearance of two kinds of perturbed terms, a scale factor spatial variation along with perturbed Hubble expansion rate. We study both the background and the perturbation evolution within the parametrized post-Friedmann scheme, obtaining that the exchange of energy-momentum can flow from dark energy to dark matter in order to keep dark energy and dark matter densities well defined at all times. We combine several measures of the cosmic microwave background (WMAP9+Planck) data, baryon acoustic oscillation measurements, redshift-space distortion data, JLA sample of supernovae, and Hubble constant for constraining the coupling constant and the exponent provided both parametrized the interaction itself. The joint analysis of Planck + WMAP9 + BAO +RSD + JLA + HST data seems to favor large interacting coupling, $\xi_c = 0.34403427^{+0.14430125}_{-0.18907353}$ at 1 σ level, and prefers a power law interaction with a negative exponent, thus $\beta = -0.50863232^{+0.48424166}_{-0.40923857}$ at 1 σ level. The CMB temperature power spectrum indicates that a large coupling constant produces a shift of the acoustic peaks and affects their amplitudes at lower multipoles. In addition, a larger β exponent generates a shift of the acoustic peaks, pointing a clear deviation with respect to the concordance model. The matter power spectrum are sensitive to the variation of the coupling constant and the β exponent. In this context, the interaction alters the scale of matter and radiation equality and pushes it away from the present era, which in turn generates a shift of the turnover point toward to smaller scale.

PACS numbers: 98.80.-k, 98.80.Es

I. INTRODUCTION

Our current view of the Universe is based on the large amount of cosmological observations provided by several surveys [1], [2], [3]. In particular, the first released data by Planck mission seem to indicate that our Universe is filled with two dark components representing the 95 % of the cosmic budget [4], [5], [6], in fact, these components are non-baryonic in nature. On one side, dark energy can be treated as a fluid with negative pressure which violates the strong energy condition, counter-balancing the net gravity effect on the large scale by driven the Universe toward an accelerated expansion era, leaving behind an earlier non-accelerated epoch. However, it was not discovered yet what is the microscopic mechanism which triggers the expansion of the Universe and therefore there is not a single fundamental theory which shows how fast this transition takes place or when exactly occurs. On the other side, dark matter can be accommodated as a pressureless fluid which helps to cluster matter and affect in this way the whole distribution of galaxies in the Universe [7], [8], [9]. Such component leaves its imprint in the power spectrum of clustered matter or through gravitational lensing of mass distribution [1], [5]. A further exploration of the clustered matter dynamic needs to include observations that account for the behavior of dark matter perturbation and its clustering effect on sub-Hubble scale. A useful manner to achieve this goal is by redshift space distortion (RSD) measurements of $f\sigma_8$ quantity at different redshifts, where f is the growth rate factor and σ_8 is rms density contrast within an 8 Mpch^{-1} sphere, while h stands for the dimensionless Hubble parameter [10], [11], [12]. Given RSD measurements are related with peculiar velocities of galaxies, the use $f\sigma_8$ data is considered as a promising way to test a cosmological model beyond the background level, helping to break the degeneracy between different parameters [13], [14], [15], [16].

A pressing issue of modern cosmology relies on the existence of non vanishing interaction between dark matter and dark energy. This phenomenon is not only consistent with recent Planck cosmological data [17], [18], [19], but also seems to be possible at theoretical level when

*Electronic address: martin@df.uba.ar
†Electronic address: lxxu@dlut.edu.cn (corresponding-author)

coupled scalar fields are considered [20], [21], [22], [23]. A signature of the exchange of energy in the dark sector can be searched in different manners, for instance, a starting point is to explore the behavior of dark energy density at early time [24] along with the amount of dark energy at the recombination epoch [5], [25], [26]. Another interesting route is to examine the impact of the cosmological constraints over an interacting dark energy model when a dynamical probe such as RSD measurements are included [19]. As an exmple, a geometric (background) test based on CMB + BAO + SNe data for an interaction proportional to dark matter density seems to avoid large coupling, leading to a coupling constant $\xi_c = 0.0013 \pm 0.0008$ at 1σ level [27]. The inclusion of RSD measurements improves a little bit this constraint provided the joint statistical analysis performed with CMB + BAO + SNe + RSD data leads to $\xi_c = 0.00140^{+0.00079}_{-0.00080}$ at 1σ level [28]. Even though the latter result differs from the former one, we notice that the disagreement is not bigger than 0.022%. In the light of previous outcome, one might wonder if the small value of the coupling constant can be extrapolated as a general output of interacting dark energy models when dark matter and dark energy are both treated as fluids. Contrary to the previous results, Salvatelli *et al.* found that a piecewise vacuum interaction, with a large negative coupling constant, is favored at late time by the joint analysis of Planck + Union2.1 + RSD + BAO data [29]. The latter result would show that the coupling constant strenght depends on several factors, that is, it is likely linked with the specific form of the interaction, the data selected for implementing a statistical analysis, and above all it is not only connected with the underlying framework used for treating the dark components [28].

In this work, we are going to explore an alternative interaction between dark matter and dark energy which is parametrized as a product of the Hubble function and a scale factor power law up to a coupling constant. We will include linear perturbations into the cosmic constraint with the help of the parametrized post-Friedmann (PPF) formalism [30], [31], [32] for avoiding non-adiabatic instabilities which could happen within the framework of an interacting dark sector [27], [33], [34], [35]. We are going to assess how the interaction affects the background evolution along with its impact on the perturbation equations in the IPPF scheme [27], [28]. We will analyze how the cosmic parameters are affected by this exchange of energy taking into account that the perturbed fluid equations will admit a perturbed interaction which have both spatial variation of the scalar factor along with perturbed Hubble expansion rate. We will consider a momentum transfer potential corresponding to an interaction vector proportional to dark matter velocity in order to avoid a violation of the weak equivalence principle. We will perform a MCMC statistical analysis by modifying CosmoMC package [36]. Our analysis will rely on different observational probes such supernovae Ia from JLA sample, BAO, HST, Planck+WMAP plus a dynamical test based on RSD measurements. We also will explore the TT power spectrum of cosmic microwave radiation and the power spectrum of clustered matter by running a modified version of the CAMB code [37], focusing on the behavior of both magnitudes when the coupling constant varies.

II. BACKGROUND AND PERTURBATION EQUATIONS

A. Background

We assume a spatially flat Friedmann-Robertson-Walker background described by the metric $g_{\mu\nu} = a^2 \mathrm{diag}[-1, \gamma_{ij}]$ with local coordinates (η, x^i), where the conformal time is defined as $d\eta = a^{-1}dt$, and γ_{ij} stands for the the spatial metric. Einstein equations, $G_{\mu\nu} = \kappa T_{\mu\nu}$ with $\kappa = 8\pi G$, lead to Friedmann constraint:

$$H^2 + \frac{K}{a^2} = \frac{\kappa}{3}(\rho_T + \rho_x)\,. \tag{1}$$

As is customary, the continuity equations for total matter (dark matter, baryons, neutrinos) and effective dark energy are given by

$$\begin{aligned} \rho_T' &= -3(\rho_T + p_T) + \frac{Q_c}{H}\,, \\ \rho_x' &= -3(\rho_x + p_x) + \frac{Q_x}{H}\,, \end{aligned} \tag{2}$$

when dark matter and effective dark energy are coupled. For simplicity, we assume a phenomenological interaction that can be parametrized in terms of two constants only and that the form of the coupling between dark components is of a power law form for concreteness: $Q_x = H\bar{Q}_x$ with $\bar{Q}_x = -\xi_c \rho_{c0} a^\beta$. We solve background equations for the interacting dark sector [38]:

$$\begin{aligned} \rho_x &= \rho_{x0} a^{-3(1+w_x)} - \frac{\xi_c \rho_{c0}}{3(1+w_x)+\beta} a^\beta\,, \\ \rho_c &= \rho_{c0} a^{-3(1+w_c)} + \frac{\xi_c \rho_{c0}}{3(1+w_c)+\beta} a^\beta. \end{aligned} \tag{3}$$

As an illustration, we write the cold dark matter density as the product of its density by its mass, $\rho_c = n_c m_c(a)$, and we realize that the mass of cold dark matter particle is no longer constant but it varies with the cosmic time:

$$m_c(a) = \rho_{c0}\Big(1 + \frac{\xi_c}{3\beta} a^{\beta+3}\Big). \tag{4}$$

At this point we would like to emphasize that dark matter and dark energy are both treated as fluids because the true nature of these dark components is not known yet provided the degree of freedoms which describe them have not been discovered so far. Furthermore, an interaction like we have proposed might not have a simple identification in terms of a coupled quintessence model [20],

[21], [22], [23]. Now, we focus on the possible choices that the parameter space would admit and make some comments about these cases. In the case of $w_c = 0$ and $\xi_c > 0$, the parameter space is defined through the conditions $\beta > -3$ and $w_x < -(1+\beta/3) < 0$, which allow us to have positive energy density at all times. Another possible branch corresponds to taking $w_c = 0$ and $\xi_c < 0$ in the background equations (3), however, this case leads to an unphysical conditions $w_x > 0$. In short, the interaction proposed here only allows to have an exchange of energy-momentum from dark energy to dark matter ($\xi_c > 0$) in order to keep the energy densities as positive definite quantities for all times. Besides, the vanilla model can be obtained when the coupling constant vanishes together with the choices $w_c = 0$ and $w_x = -1$.

B. Perturbation

As we are interested in analyzing the behavior of scalar linear perturbation, we have to perturb the Einstein equation and balance equations around a FRW background. To do that, we conveniently write the perturbed variables as a linear combination of the eigenfunction (plane-wave) $Y(\mathbf{x})$ of the Laplace operator [39], [40]. At the end, the perturbed metric is characterized by four functions called potential A, shift B, curvature H_L, and shear H_T:

$$\begin{aligned}&\delta g_{00} = -a^2(2AY)\,,\ \delta g_{0i} = -a^2 B Y_i\,,\\ &\delta g_{ij} = a^2(2H_L Y\gamma_{ij} + 2H_T Y_{ij})\,.\end{aligned} \tag{5}$$

Here Y_i stands for the covariant derivative of the eigenfunction $Y(\mathbf{x})$. The perturbed energy-momentum tensor involves isotropic and anisotropic pressure perturbations, density, and velocity perturbations:

$$\begin{aligned}&\delta T^0{}_0 = -\delta\rho\,,\ \delta T_0{}^i = -(\rho+p)vY^i\,,\\ &\delta T^i{}_j = \delta p Y\delta^i{}_j + p\Pi Y^i{}_j\,.\end{aligned} \tag{6}$$

The Einstein equations can be written as

$$\begin{aligned}&H_L + \frac{1}{3}H_T + \frac{B}{k_H} - \frac{H_T'}{k_H^2} = \\ &\frac{\kappa}{2H^2 c_K k_H^2}\left[\delta\rho + 3(\rho+p)\frac{v-B}{k_H}\right]\,,\\ &A - H_L' - \frac{H_T'}{3} - \frac{K}{(aH)^2}\left(\frac{B}{k_H} - \frac{H_T'}{k_H^2}\right)\\ &= \frac{\kappa}{2H^2}(\rho+p)\frac{v-B}{k_H}\,,\end{aligned} \tag{7}$$

where the prime refers to a logarithmic derivative, $k_H = (k/aH)$, $c_K = 1 - 3K/k^2$, and K is the spatial curvature. In order to further illustrate how the perturbation theory works, we need to propose a covariant four-vector interaction, $Q^\nu{}_I$, which encodes the transfer of energy and momentum:

$$\nabla_\nu T^{\mu\nu}_I = Q^\nu{}_I, \qquad \sum_{I=x,c} Q^\nu{}_I = 0\,. \tag{8}$$

Then, we have a perturbed continuity and a perturbed Navier-Stokes equation for each fluid

$$\begin{aligned}&(\rho_i\Delta_i)' + 3(\rho_i\Delta_i + \Delta p_i) + (\rho_i + p_i)(k_H V_i + 3H_L')\\ &= \frac{\Delta Q_i - \xi Q_i}{H}\,,\\ &\frac{[a^4(\rho_i+p_i)(V_i - B)]'}{a^4 k_H} - \Delta p_i + \frac{2}{3}c_K p_i\Pi_i - (\rho_i+p_i)A\\ &= \frac{a}{k}[Q_i(V - V_T) + f_i]\,.\end{aligned} \tag{9}$$

For scalar perturbations (5), the perturbed velocity vector becomes $u_{\nu\ I} = a\big[-(1+AY); (V_I - B)Y_i\big]$, which means the four vector interaction can be written as

$$Q_{\nu\ I} = a\big(-Q_I(1+YA) - \delta Q_I Y; [F_I + Q_I(V-B)]Y_i\big)\,, \tag{10}$$

where δQ_I and F_I stand for the energy transfer perturbation and the intrinsic momentum transfer potential of I-fluid, respectively. The conservation of total energy-momentum for dark components implies that

$$Q_c = -Q_x, \quad F_c = -F_x, \qquad \delta Q_c = -\delta Q_x.$$

C. The PPF method

To apply the PPF method we must make some assumptions about the behavior dark energy perturbations on super-horizon scales, that is, the effective dark energy contribution in the large scale limit ($k_H \to 0$) must be accommodated in terms of a single function $f_\zeta(a)$ [31]:

$$\lim_{k_H \ll 1} \frac{\kappa}{2H^2}(\rho_x + p_x)\frac{V_x - V_T}{k_H} = -\frac{1}{3}c_K f_\zeta(a) k_H V_T\,. \tag{11}$$

Here we implicitly assumed to be working in the co-moving gauge ($B = V_T$, $H_T = 0$) where we called $A = \xi$, $H_L = \zeta$. Further, the derivative of curvature perturbation becomes

$$\begin{aligned}\lim_{k_H \ll 1}\zeta' = &-\frac{\frac{a}{k}[Q_c(V - V_T) + f_c] + \Delta p_T - \frac{2}{3}c_K p_T\Pi_T}{(\rho_T + p_T)}\\ &- \frac{K}{k^2}k_H V_T + \frac{1}{3}c_K f_\zeta k_H V_T\,,\end{aligned} \tag{12}$$

so the PPF method deals with $\zeta' \simeq 0$ in the co-moving gauge, consequently dark energy fluctuations become important at second order in the co-moving wave number $k_{\rm H}$ (cf.[31]) provided $k_H V_T = \mathcal{O}(k_H^2\zeta)$. From now on, we are going to neglect any contribution from anisotropic pressure terms for total matter and effective dark energy, $\Pi_T = \Pi_x = 0$.

The behavior of the gravitational potential is related with the evolution of curvature perturbation by means of $\Phi = \zeta + V_T/k_H$. In fact, the potential must fulfill a Poisson-like equation in the quasi-static limit: $\Phi(k_H \gg 1) = \kappa a^2 \Delta_T \rho_T / 2k^2 c_K$. The PPF prescription relies on the simple fact that the behavior of curvature perturbations on the two different scales must be linked by means of a single degree of freedom encoded in the Γ function [31] as follows:

$$\Phi + \Gamma = \frac{\kappa a^2}{2c_K k^2} \Delta_T \rho_T. \tag{13}$$

In the large-scale limit, we obtain $\Gamma' = S - \Gamma$, where the source term can be recast as

$$S = \frac{\kappa a^2}{2k^2}\Big(\frac{3a}{kc_K}[Q_c(V - V_T) + F_c] + \frac{1}{Hc_K}[\Delta Q_c - \xi Q_c] + V_T k_H[-f_\zeta(\rho_T + p_T) + (\rho_x + p_x)]\Big) . \tag{14}$$

In order to link the behavior of perturbed quantities at different scales, we must introduce a master equation for Γ:

$$(1 + c_\Gamma^2 k_H^2)[\Gamma' + \Gamma + c_\Gamma^2 k_H^2 \Gamma] = S\,, \tag{15}$$

where the condition $c_\Gamma k = \mathcal{H}$ determines the transition between large scale regime and the quasi-static phase, that is, the PPF method introduces a new parameter called c_Γ. In regard to the initial condition for Γ, we take a vanishing Γ at small scale factor provided the source term goes to zero in this limit.

So far we have been working with the function Γ in order to connect two separated scales, but we have not said anything about how we deal with dark energy perturbations in the previous method. The crucial fact of the PPF method is that forces dark energy density perturbations to remain smaller than the dark matter perturbation [31]. In doing so, one does not give a closure relation between dark energy pressure perturbation and dark energy density perturbation because one would like to avoid the appearance of large-scale instabilities [27], [28]. As a result, the perturbed dark energy density and peculiar velocity are both derived once the new dynamical function is known (cf. [28], [31]):

$$\rho_x \Delta_x + 3(\rho_x + p_x)\frac{V_x - V_T}{k_H} = -\frac{2k^2 c_K}{\kappa a^2}\Gamma\,, \tag{16}$$

$$\kappa a^2 V_x(\rho_x + p_x) = -\frac{2a^2\mathcal{H}k}{F(a)}\Big([S_0 - \Gamma - \Gamma'] + \frac{\kappa a^2}{2k^2} f_\zeta(\rho_T + p_T) V_T k_H\Big) + \kappa a^2 V_T(\rho_x + p_x)\,, \tag{17}$$

where $F(a) = 1 + 3\frac{\kappa a^2}{2k^2 c_K}(\rho_T + p_T)$. Here we are keeping only the leading terms in the source expression for small comoving wave number k_H, and we are calling this result S_0 [28].

In this study, we will be concerned with the physical consequences coming from the IPPF method when an interaction four-vector can be written as $Q_x^\mu = H\bar{Q}_x u_c^\mu$ with $\bar{Q}_x = -\xi_c \rho_{c0} a^\beta$ and $Q_x \equiv a Q_x^0 = H\bar{Q}_x$. In this case, the interaction is given by

$$Q_{\nu\ x} = a\bar{Q}_x H\big[-(1 + AY); (V_c - B)Y_i\big]\,. \tag{18}$$

From (10) and (18), we obtain that the perturbed interaction can be written as

$$\delta Q_x = \delta H \bar{Q}_x(a) + H\bar{Q}'_x(a)\delta a\,, \tag{19}$$

while for the momentum transfer potential we find that $F_x = Q_x(V_c - V) = -F_c$ provided $Q_c^\mu || u_c^\mu$, avoiding in this way the violation of weak equivalence principle [28]. Notice that δQ_x contains two different kinds of terms, namely δQ_x receives contributions from the spatial variation of H and the spatial variation of the scale factor. In order to carry on and explore the impact of this new interaction on the parameter space, it is essential to modify or include several routines in the numerical code called CAMB. Given that this code is written in the synchronous gauge we need to handle all these expressions into this gauge characterized by $A = B = 0$. Replacing both conditions into gauge transformation for metric variables indicates that scalar perturbations can be treated in terms of two functions: $\eta_T \equiv -\frac{1}{3}H_T - H_L$ and $h_L = 6H_L$ [28]. From the later fact, with the help of the metric (5), we calculate δH and δa in the synchronous gauge as

$$\begin{aligned}[\delta a]_{\rm syn} &= -a(\eta_T - \mathcal{H}\sigma)\,,\\ [\delta H]_{\rm syn} &= -\frac{1}{a}[\dot{\eta}_T + \sigma(\mathcal{H}^2 - \dot{\mathcal{H}})],\end{aligned} \tag{20}$$

where $\sigma = (\dot{h}_L + 3\dot{\eta}_T)/2k^2$ and the overdot refers to conformal time derivative. Combining Eqs. (20) and Eq. (19) in the synchronous gauge, we have

$$\delta Q_x = \frac{\bar{Q}_x}{a}[\dot{\eta}_T + \beta\mathcal{H}\eta_T + \sigma(\mathcal{H}^2 - \beta\mathcal{H}^2 - \dot{\mathcal{H}})]. \tag{21}$$

To understand the cosmological constraints performed with redshift space distortion measurements we must give further insights about the dynamical evolution of dark matter perturbations. We need to examine if the exchange of energy-momentum in the dark sector may alter the standard Euler and continuity equations for dark matter, leading to a detectable signature about its dynamic in relation with the behavior of galaxies. Our starting point is to calculate the evolution equations for the perturbation of cold dark matter in the synchronous gauge [28]:

$$\dot{\delta}_c + \theta_c + \frac{\dot{h}_L}{2} = \frac{a}{\rho_c}[\delta Q_c - \delta_c Q_c], \tag{22}$$

$$\dot{\theta}_c + \theta_c\mathcal{H} = \frac{a}{\rho_c}[Q_c(\theta - \theta_c) - k^2 F_c], \tag{23}$$

where we used that the adiabatic sound speed defined as $c_{ac}^2 = \dot{p}_c/\dot{\rho}_c = w_c + \dot{w}_c/(\dot{\rho}_c/\rho_c)$ vanishes, $w_c = 0$, and the physical sound speed in the rest frame, namely $c_{sc}^2 = (\delta p_c/\delta\rho_c)_{\text{rest frame}} = 0$ for cold dark matter, and the density contrast is defined as $\delta_c = \rho_c\Delta\rho_c/\rho_c$. For the definition of θ_c and θ see our previous article [28].

After decoupling, the baryons do not interact with the dark sector so its Euler and continuity equations within the synchronous gauge are given by

$$\dot{\delta}_b + \theta_b + \frac{\dot{h}_L}{2} = 0, \tag{24}$$

$$\dot{\theta}_b + \theta_b\mathcal{H} = 0. \tag{25}$$

In our case, we find $[Q_c(\theta - \theta_c) - k^2F_c] = 0$ provided the momentum transfer potential is $-k^2F_c = Q_c(\theta_c - \theta)$. This implies that the Euler equation for dark matter is not altered in relation with the non-interacting case. As a result, we obtain that the difference between Euler equations (23-25) leads to $(\dot{\theta}_c - \dot{\theta}_b) = -\mathcal{H}(\theta_c - \theta_b)$, and therefore we can assure that there is no velocity bias within this model [41]. This fact pinpoints that dark matter velocity is not directly affected by the interaction, which means that dark matter follows geodesic and there is not violation of the weak equivalence principle [42].

Combining Eq. (22) for $\dot{\delta}_c$ along with the Einstein equations in the synchronous gauge [40], we arrived at the second-order evolution equation for dark matter perturbation:

$$\ddot{\delta}_c + \mathcal{H}\dot{\delta}_c\Big(1 + \frac{aQ_c}{\rho_c\mathcal{H}}\Big) =$$

$$4\pi Ga^2\Big[\delta_b\rho_b + \delta_c\rho_c\Big(1 - \frac{(\rho_c^{-1}Q_c)^{\cdot}}{4\pi Ga\rho_c}\Big)\Big] + a\Big(\frac{\delta Q_c}{\rho_c}\Big)^{\cdot}. \tag{26}$$

The growth of dark matter perturbations are affected in a number of ways. Firstly, the modification of the dark matter contrast density enters through the expansion history encoded in the Hubble expansion and cold dark matter density, which will lead to a faster or slower clustering of matter particles according to the values taken by ξ_c and β. Secondly, the friction term of Eq. (26) is altered by the extra contribution, $aQ_c/\rho_c\mathcal{H}$, implying that the rate growth will depend both on Q_c and the background evolution described by $\mathcal{H}$. Thirdly, the cold dark matter particle feel and additional force that is mediated by dark energy particle described by an effective gravitational constant. As cold dark matter particles have a mass which varies with time, the uncoupled baryons will feel this effect through a changing gravitational potential. It is clear that the extra-term in Eq. (26) is related with the fact that δQ_c cannot be recast as $\delta\rho_c Q_c$ provided our interaction is no proportional to ρ_c. At this point, we must highlight the importance of dark matter perturbations and baryon perturbations, both contributions are essentials for understanding the formation of the large-scale structure of the Universe. More precisely, the growth data involve the linear perturbation of the overall growth factor $\delta_{\rm m}$ in terms of the function $f_m = d\ln\,\delta_{\rm m}/d\ln\,a$ along with the r.m.s density contrast within an sphere of radius $R_8 = 8$Mpc h^{-1}, which is related with the matter power spectrum. As explained before, the measurements of redshift space distortions lead to a bias-independent quantity called $f(z)\sigma_8(z)$ [15] and is used it as a powerful tool for improving the cosmological constraints beyond the background probes based on supernovae data. It is possible to use these data in our cosmic constraint but we must first modify the CAMB code for extracting the theoretical value of $f(z)\sigma_8(z)$, and such procedure involves to re-write different routines. On one side, $\sigma_8(z)$ is given by

z	$f\sigma_8(z)$	survey
0.067	0.42 ± 0.06	6dFGRS (2012)
0.17	0.51 ± 0.06	2dFGRS (2004)
0.22	0.42 ± 0.07	WiggleZ (2011)
0.25	0.39 ± 0.05	SDSS LRG (2011)
0.37	0.43 ± 0.04	SDSS LRG (2011)
0.41	0.45 ± 0.04	WiggleZ (2011)
0.57	0.43 ± 0.03	BOSS CMASS (2012)
0.60	0.43 ± 0.04	WiggleZ (2011)
0.78	0.38 ± 0.04	WiggleZ (2011)
0.80	0.47 ± 0.08	VIPERS (2013)

TABLE I: Compilation of $f\sigma_8(z)$ data points obtained from several galaxy surveys using RSD method.

$$\sigma_8(z) = \left[\frac{1}{2\pi^2}\int_0^\infty dk k^2 W_8^2(k)P(k,z)\right]^{1/2}, \tag{27}$$

where $W_8(k)$ is the Fourier transform of the top-hat window function, with an interval defined by R_8, and $P(k,z)$ refers to the matter power spectrum. It can be seen that in our model the overall growth matter rate is

$$f_m(a) = \frac{\rho_c\delta_c' + \rho_b\delta_b'}{\mathcal{H}(\delta_c + \rho_b)} + \frac{\xi_c\rho_{c0}a^\beta}{\rho_c + \rho_b}\left(\frac{\delta_c}{\delta_m} - 1\right), \tag{28}$$

where the interaction induces an extra term which plays the role of a relative weight between cold dark matter contrast density and total matter contrast density. Moreover, (28) shows that the interaction reduces the overall growth matter rate for positive coupling constant, $\xi_c > 0$. This difference therefore must leave to a detectable signature, which allows differentiation between previous works [28], [44] .

III. CONSTRAINT AND RESULTS

We perform a statistical estimation of the cosmic parameters by using the Markov Chain Monte-Carlo method with help of public code CosmoMC [36] and CAMB code [37]. In order to do so, we add a new module to CosmoMC package for taking into account the value

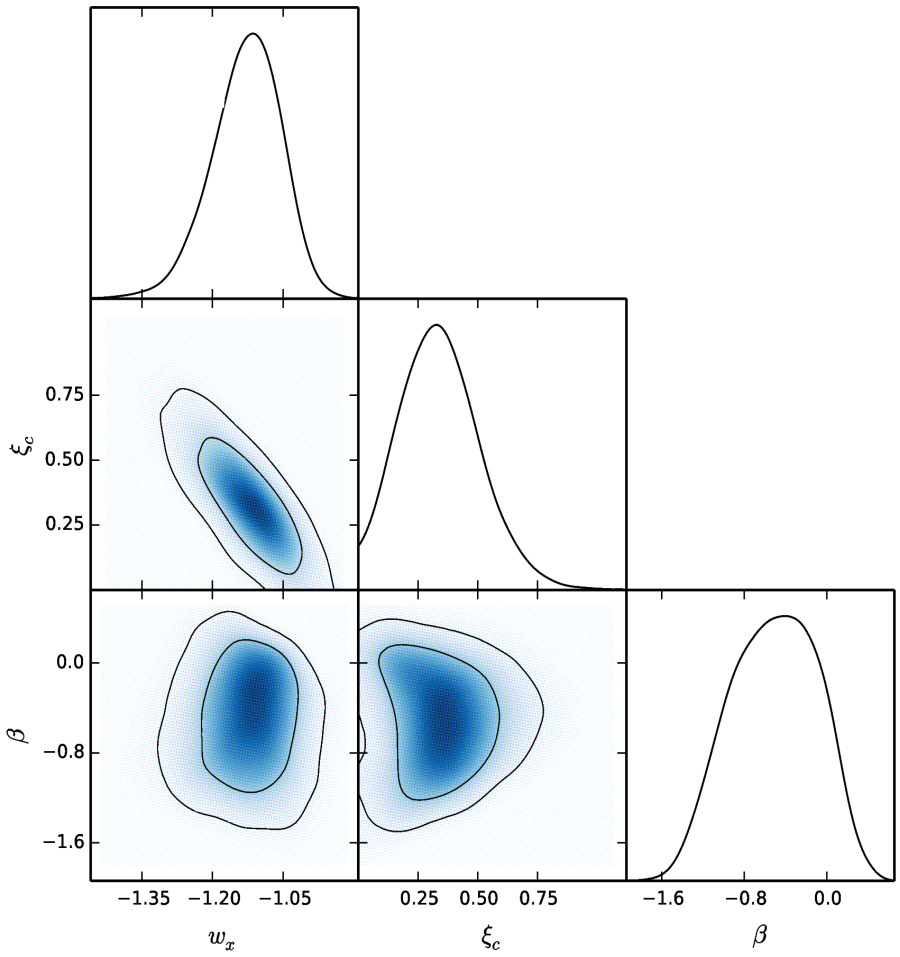

FIG. 1: 68 % and 95 % constraints on w_x, ξ_c, and β from the combined analysis made with the Planck 2013+WMAP9+JLA+BAO+RSD+HST data. The 1D marginalized posterior distribution of w_x, ξ_c, and β are also shown.

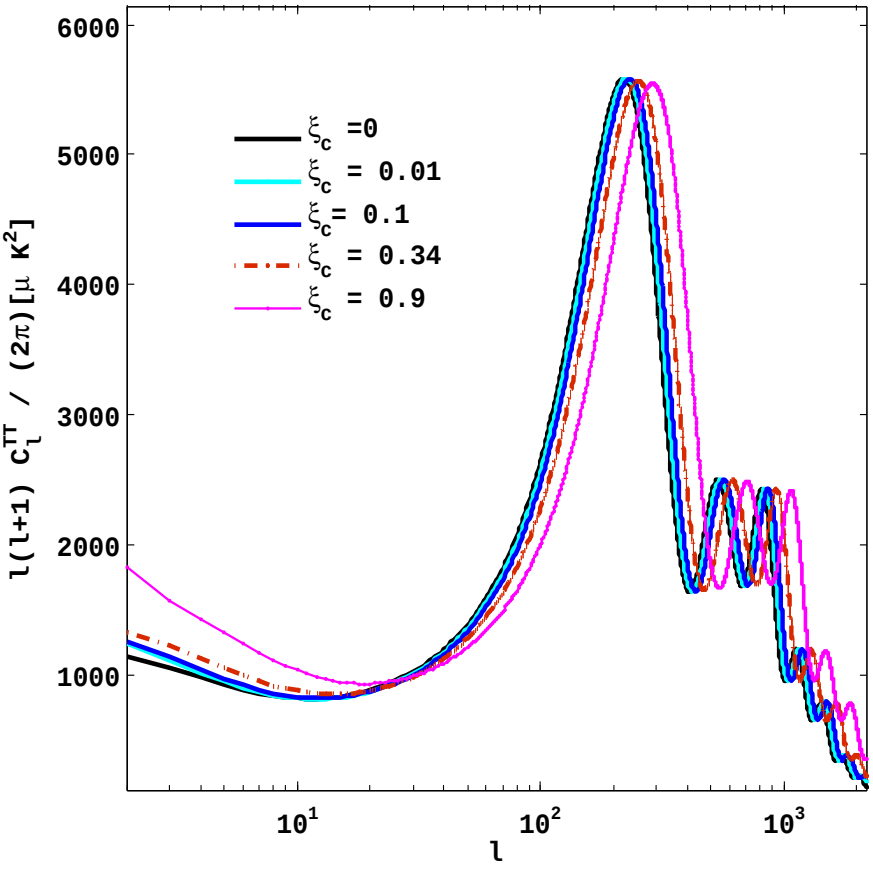

FIG. 2: Typical effects of the coupling constant on the theoretical CMB temperature power spectrum. We exhibit $C_{\rm l}^{\rm TT}$ versus multipole for different values of the coupling constant.

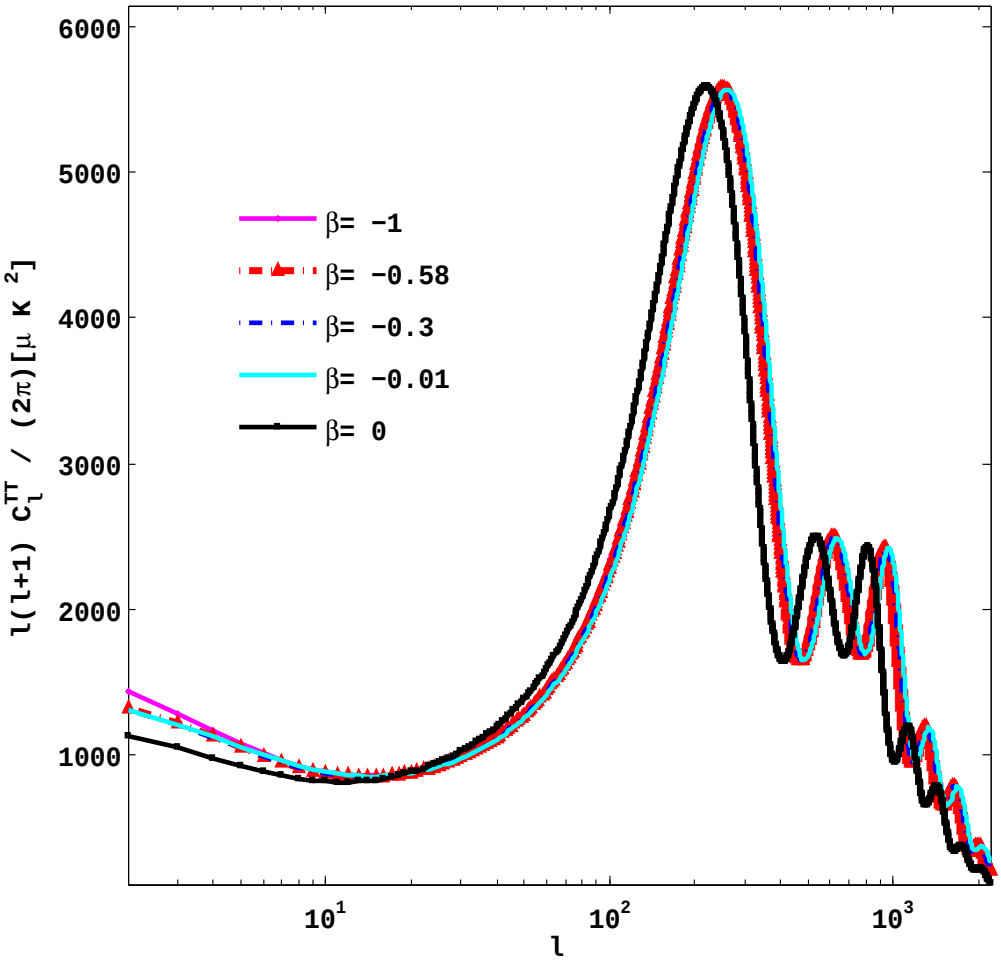

FIG. 3: Typical effects of the β exponent on the theoretical CMB temperature power spectrum. We show C_l^{TT} versus multipole for different power-law interactions.

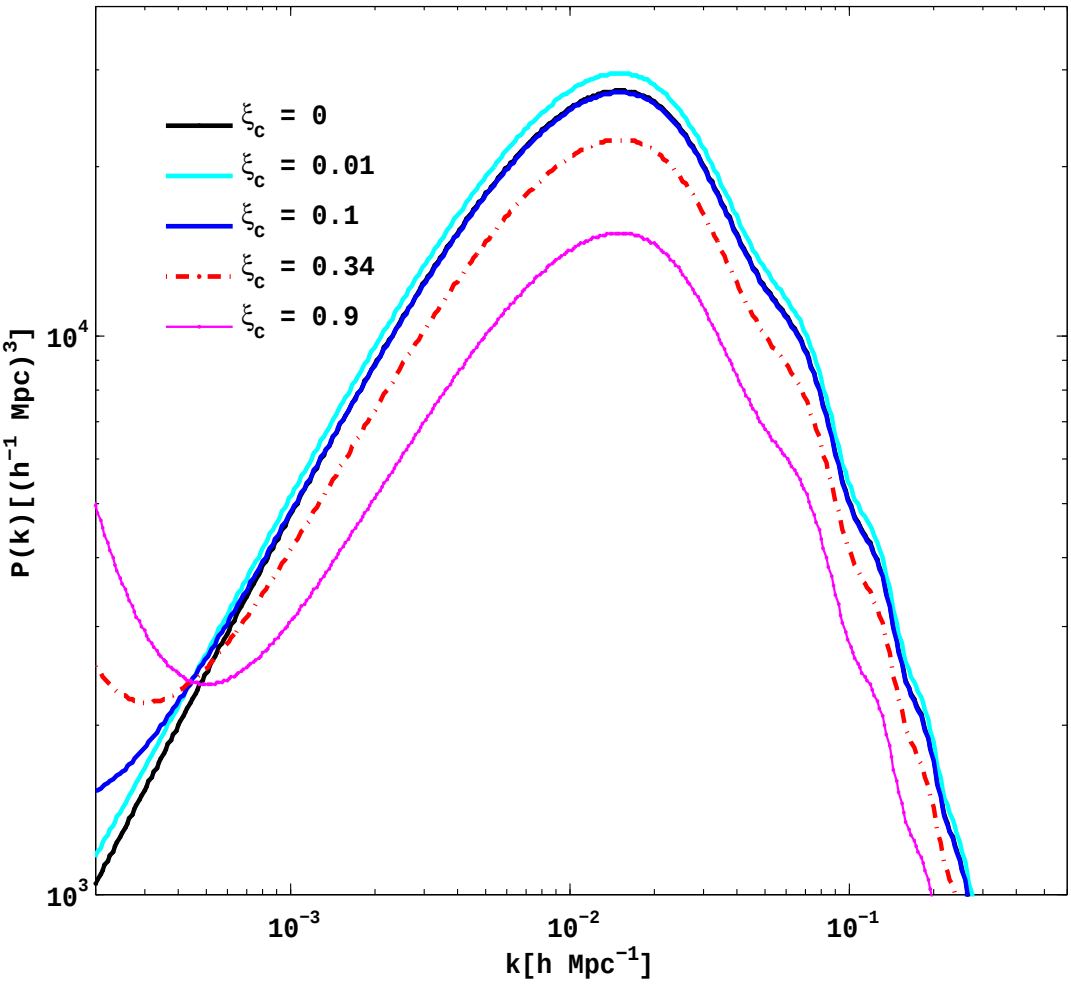

FIG. 4: The total matter power spectrum at $z = 0$ as the coupling constant varies from 0 to 0.9. Baryon acoustic oscillations generate wiggles in the matter power spectrum.

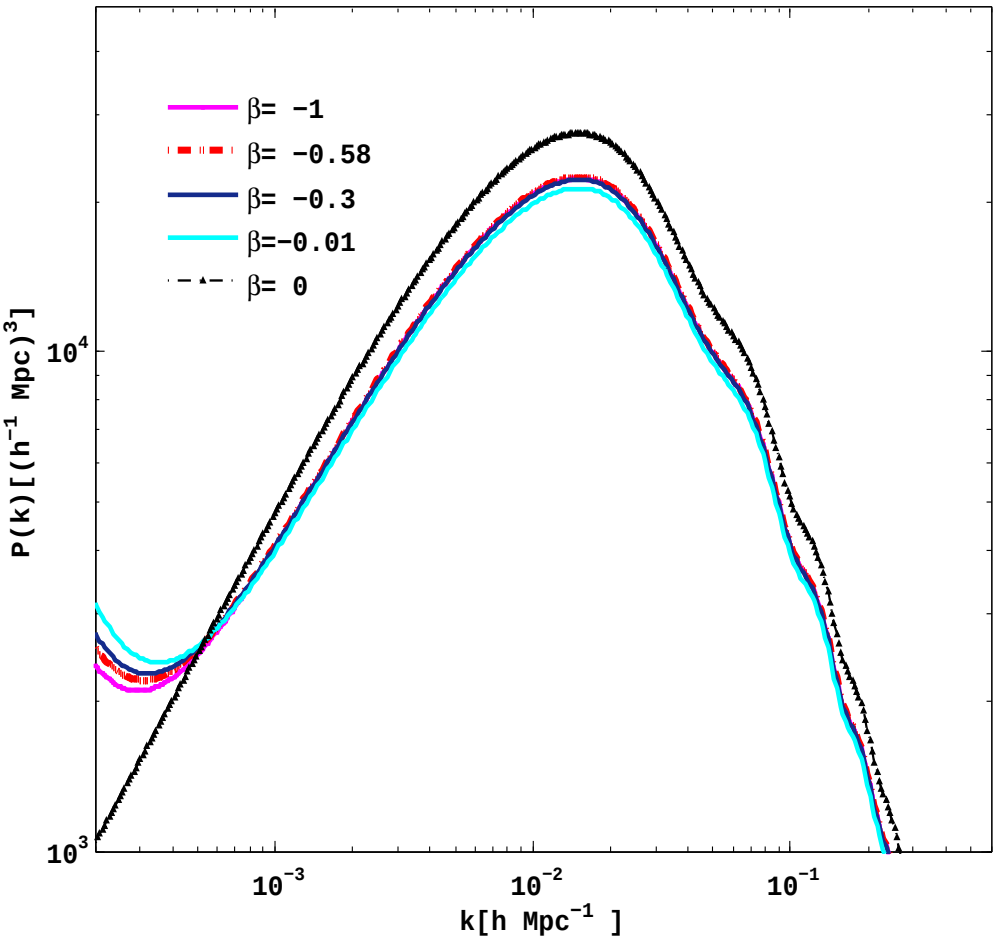

FIG. 5: The total matter power spectrum at $z = 0$ as the β exponent varies from 0 to -1. Baryon acoustic oscillations generate wiggles in the matter power spectrum.

Parameters	Mean with errors	Best fit
$\Omega_b h^2$	$0.02215594^{+0.00025836}_{-0.00026246}$	0.02222252
$\Omega_c h^2$	$0.11864910^{+0.00196349}_{-0.00211040}$	0.11845120
$100\theta_{MC}$	$1.04143237^{+0.00058065}_{-0.00057134}$	1.04152800
τ	$0.08910617^{+0.01235947}_{-0.01346580}$	0.08779789
w_x	$-1.12874223^{+0.08205012}_{-0.06244387}$	-1.14908200
ξ_c	$0.34403427^{+0.14430125}_{-0.18907353}$	0.32413630
β	$-0.50863232^{+0.48424166}_{-0.40923857}$	-1.06008500
$\ln(10^{10}A_s)$	$3.08464588^{+0.02442454}_{-0.02425935}$	3.08247800
n_s	$0.96269367^{+0.00624026}_{-0.00622752}$	0.96447760
H_0	$63.68287359^{+3.34545416}_{-2.30201737}$	65.75439000
Ω_x	$0.64884118^{+0.04222175}_{-0.02299489}$	0.67314830
Ω_m	$0.35115882^{+0.02299549}_{-0.04222199}$	0.32685170
$\Omega_m h^2$	$0.14145019^{+0.00187374}_{-0.00201151}$	0.14131890
σ_8	$0.76985212^{+0.02336652}_{-0.02119374}$	0.78026930
Age/Gyr	$13.77835552^{+0.03828760}_{-0.03804099}$	13.78876000
z_*	$1090.05905721^{+0.44064201}_{-0.43505566}$	1089.95200000
r_*	$144.94953514^{+0.47179303}_{-0.47690640}$	144.94740000
θ_*	$1.04165139^{+0.00057374}_{-0.00056187}$	1.04174300

TABLE II: Statistical results from the global fitting performed with the Planck 2013+WMAP9+JLA+BAO+RSD+HST data.

of f_m obtained with the CAMB code, in this way, we calculate the theoretical value of $f(z)\sigma_8(z)$ at different redshift, compare with their observational value, and build the χ^2 likelihood for performing a statistical estimation on the parameter space [43]. Two comments are in order concerning the PPF "parameters". When c_Γ is taken as free model parameter one finds that its posterior probability distribution has a flat shape, showing that any value between zero and the unity are physically admissible [28], in fact, a similar analysis can be obtained for the function f_ξ [31]. The list of the cosmological data used for our parameter estimations (cf. [28] for further details about the methodology) are:

- SNeIa, JLA data: 740 supernovae samples from low redshift $z = 0.02$ to large one $z \simeq 1$, obtained from the joint analysis of SDSS II and SNLS [3].
- CMB, WMAP9 + Planck: multipole measurements obtained by WMAP9 team [2] and Planck satellite [4], [5], [6]. WMAP9 project involves the measurements of Atacama Cosmology Telescope (ACT) at high multipoles, $\ell \in [500, 10000]$, along with the South Pole Telescope (SPT) observations which reported data over the range $\ell \in [600, 3000]$. Planck survey performed measurements over a complementary zone, $\ell \in [2, 2500]$.
- BAO, DR9 − DR7 − 6dFGS: the 6dFGS mission reported $d_z(0.106)$ [7], SDSS-DR7 measured $d_z(0.35)$ [8], SDSS-DR9 exploration led to $d_z(0.57)$ [9], and diverse measurements from the Wiggle Z dark energy survey reported $d_z(0.44)$, $d_z(0.60)$, and $d_z(0.73)$.
- HST, Hubble: Gaussian prior for H_0.
- RSD, Growth data: measurements of the quantity $f(z)\sigma_8(z)$ at different redshifts unify the cosmic growth rate f and the matter power spectrum σ_8 normalized with the co-moving scale $8h^{-1}$ Mpc, in a single quantity which includes the latest results of galaxy surveys such as 6dFGS, BOSS, LRG, Wiggle Z, and VIPERS [see Table (I)].

The parameter space is given by [28]

$$\mathcal{P} = \Big(\Omega_b h^2, \Omega_c h^2, 100\theta_{\rm MC}, {\rm n_s}, \ln(10^{10}{\rm A_s}), \tau, w_x, \xi_c, \beta\Big), \tag{29}$$

and each data base is taken as independent one, so the likelihood distribution is

$$\chi^2_{\rm total} = \chi^2_{\rm SNe} + \chi^2_{\rm BAO} + \chi^2_{\rm CMB} + \chi^2_{\rm HST} + \chi^2_{\rm RSD}. \tag{30}$$

Let us analyze the outcome of our statistical analysis obtained by combining all Planck2013 + WMAP9 + JLA + BAO + HST + RSD data [see Table (II)]. The equation of state of dark energy is given by $w_x = -1.12874223^{+0.08205012}_{-0.06244387}$ at 1σ level, such values confirm that the observational data prefer a phantom-like equation of state over a non-phantom one [see Fig. (1)]. Regarding the amount of dark matter at present time we find that the best fit to all data combined: $\Omega_m = 0.35115882^{+0.02299549}_{-0.04222199}$ at 1σ level, while, the Planck + WP data leads to $\Omega_m = 0.315^{+0.016}_{-0.018}$, then the disagreement is not bigger than 0.11%, moreover, comparing with the Planck 2015 data we obtain a relative difference near 0.22% for the Planck EE+lowP [45]. The best fit for dark energy amount is $\Omega_x = 0.64884118^{+0.04222175}_{-0.02299489}$ at 1σ level, showing a deviation of 0.05% in relation with the value reported by Planck mission [6]. This result is utterly consistent with the interacting cosmology explored here because the transfer of energy goes from dark energy to dark matter, then we can expect that such mechanism increases the current value of dark matter. Further, the dynamical probe included in the statistical analysis clearly shows that the overall growth rate of matter (28) is quite sensitive to the interaction proportional to the current dark matter amount. In this regard, the joint analysis of Planck2013 + WMAP9 + JLA + BAO + HST + RSD data [see Table (II) and Fig. (1)] shows that a large coupling constant cannot be ruled out in our model provided $\xi_c = 0.34403427^{+0.14430125}_{-0.18907353}$ at 1 σ level. We stress that this result depends on the addition of growth rate data and the interaction itself. More precisely, if one considers only geometric probes for performing the statistical test with CMB + BAO + SNe data, the coupling constant remains lower, near $\mathcal{O}(10^{-3})$ [27]. Despite the inclusion of the growth rate data gives a non zero deviation from the previous result, the strength of the interaction still remains small, that is, $\xi_c = 0.00140^{+0.00079}_{-0.00080}$ at 1σ level [28]. Notice that the inclusion of a perturbed expansion Hubble contribution in the standard perturbation theory does not prefer large interaction even

if growth rate data plus geometric probes are taken into account [44]. Therefore, the key point for understanding the large value of coupling constant reported here is linked with some cooperative effects coming from the inclusion of perturbed expansion Hubble rate along with spatial variation of scale factor within the interacting PPF method. Besides, the combined data of Planck2013 + WMAP9 + JLA + BAO + HST + RSD prefer a power law form with negative exponent, namely $\beta = -0.50863232^{+0.48424166}_{-0.40923857}$ at 1 σ level, indicating that the interaction is stronger in the early universe and weakens at present time. However, notice that our finding does not mean that the interaction has a vanishing contribution in the latter epoch.

The impact of the interaction can be traced by inspecting the changes introduced in the cosmic background radiation and clustered matter power spectrum, thus we explore how these quantities are affected by the two parameters which describe the interaction itself: ξ_c and β. Fig. (2) shows the CMB temperature anisotropies in terms of the multipoles for several values of the coupling constant with $\xi_c \in [0, 0.9]$. Firstly, the position of the acoustic peaks shifts to right by increasing the coupling constant. The peaks are located at $\ell_n \simeq n\pi/\theta_A$, where the acoustic scale is defined as $\theta_A = s(z_{dec})/r_{z_{dec}}$ with r known as the comoving angular diameter distance, $z_{dec} \simeq 1090$ indicates the epoch when baryons decouple from photons, and the sound horizon is given by

$$s(z) = \int_0^{1/(z+1)} c_s(a) \frac{da}{a^2 H(a)}, \tag{31}$$

where the sound speed for the photon-baryon fluid is $c_s = c/\sqrt{3(1+R)}$ and $R = 3a\Omega_b/4\Omega_r$. Since the coupling constant is positive, the exchange of energy goes from dark energy to dark matter, increases linearly the amount of dark matter at early time, affecting the sound horizon at the end, which modifies the value of the first peak located at $\ell_1 \simeq \pi/\theta_A$ as it can be seen from Fig. (2) by comparing the red-line ($\xi_c = 0.34$) with the black-line ($\xi_c = 0$). A secondary effect refers to the amplitude of CMB power spectrum at lower multipoles, it turns out that increasing the coupling constant shows a deviation from the vanilla model, so we believe that such phenomenon can be properly explored in the future by including the galaxy-ISW cross-correlated power spectrum [19]. Besides, Fig. (3) shows a shift to right in the acoustic position peaks as one moves from a vanishing exponent to a negative exponent equal to -1 while the other parameters are fixed to our best cosmology. This effect can be understood easily by taking into account that the extra-term in the cold dark matter density increases from a constant value to a^{-1}, then it amplifies the amount of dark matter at early times. It is clear that changes in the background expansion history of the Universe and modifications to the growth rate of matter perturbations will affect the matter power spectrum. In Fig. (4) we plot the matter power spectrum at $z = 0$ generated using CAMB for different values of the coupling constant, while, Fig. (5) depicts the behavior of $P(k)$ when the exponent β changes from zero to -1. Fixing all parameters to our best fit cosmology except ξ_c or the absolute value of β will have almost the same kind of impact in the matter power spectrum. The growth of density perturbations are significantly affected by the variation of β or ξ_c. This is because the amount of dark matter is bigger than the fraction of dark energy at early times when $\xi_c > 0$ and $\beta < 0$. As a result the epoch of matter-radiation equivalence happens earlier than the standard case so only the very small scale perturbations on scale $k > k_{eq}$ have time to enter the horizon and grow during the radiation domination. Hence, the most obvious effect is that the turnover in the power spectrum (which is associated with the scale that entered the horizon when the Universe became matter dominated) is placed on smaller scales. In addition, the amplitude of $P(k)$ is considerably affected as can be noticed from Figs. (4)- (5). We must stress that baryons also leave their impact on the matter power spectrum due to their coupling with the photons before recombination. Indeed, they produce a series of wiggles in the power spectrum [see Figs. (4)- (5)], which are related with the existence of a well defined peak in the correlation function of galaxies, $\xi(r)$, placed at 150 Mpc [1].

IV. SUMMARY

To avoid large-scale instability at early times associated with the growth of dark energy perturbations, we have employed the interacting PPF method for examining a new kind of interaction which includes spatial variation of Hubble function along with spatial variation of scale factor. Interestingly enough, we found that the transfer of energy-momentum can flow from dark energy to dark matter only, allowing to preserve dark energy and dark matter densities as positive quantities for all times. Concerning matter perturbations, we have shown that the overall growth rate of matter is strongly affected in three different ways. Firstly, the dark matter density and the Hubble rate at background level both deviate from the concordance model. Secondly, an extra-term related with friction in (26) reveals that the local Hubble function is modified, and thirdly the gravitational constant is amended also. The aforesaid effects are essentials for understanding the cosmological constraint based on the overall growth rate function $f_m = d\ln \delta_{\rm m}/d\ln a$ provided is connected with the measurements of redshift space distortions through a bias-independent quantity called $f(z)\sigma_8(z)$ [15].

Regarding the observational side, we performed a global fitting based on geometric and dynamical probes by combining Planck2013 + WMAP9 + JLA + BAO + RSD + HST data [see Table (II)]. The joint analysis showed that a phantom equation of state is preferred at 1 σ level and the amount of dark matter differs from the Planck

2013 estimation in 0.11% while the Planck 2015 doubles this difference after the Planck EE+lowP data is used into the analysis [45]. Such disagreement can be easily understood by taking into account that the interacting mechanism described here only allows the exchange of energy from dark energy to dark matter. Another important ingredient concerns to the particular kind of power law form selected by the data and the strength of coupling constant. More precisely, the joint analysis of Planck2013 + WMAP9 + JLA + BAO + RSD + HST data [see Table (II) and Fig. (1)] showed that a large coupling constant cannot be ruled out in our model provided, $\xi_c = 0.34403427^{+0.14430125}_{-0.18907353}$ at 1 σ level. At this point, we must note that previous estimations give a coupling constant near $\mathcal{O}(10^{-3})$ [27], [28], even though the perturbed expansion Hubble rate term is included into the analysis [44]. All the combined data (Planck2013 + WMAP9 + JLA + BAO + RSD + HST) singles out a power law form with negative exponent, $\beta = -0.50863232^{+0.48424166}_{-0.40923857}$ at 1 σ level, pinpointing the crucial effect of the interaction at early times.

We have examined how the interaction affects the temperature CMB spectrum profile, focusing in the position of acoustic peaks and their amplitudes. A similar analysis was carried out for the matter power spectrum where the target was to explore the position of turnover scale. Varying only the coupling constant, we found that the position of the first peak in the TT power spectrum is shifted because the fraction of dark matter increases linearly with ξ_c [see Fig (2)]. As the β-exponent varies only a similar effect can be pinpointed [see Fig (3)]. Besides, the amplitude of the TT CMB spectrum at low multiples is sensitive to the value taken by the coupling constant, indicating that the integrated Sachs-Wolfe must be included in a near future analysis [19]. We also found an interesting effect in the matter power spectrum by varying ξ_c or β. It turned out that the scale of matter and radiation equality is shifted further from the present era when the amount of dark matter is increased by varying ξ_c or β, and therefore a shift of the turnover point toward to smaller scale is detected [see Figs. (4)- (5)].

Acknowledgments

L.X is supported in part by NSFC under the Grants No. 11275035 and "the Fundamental Research Funds for the Central Universities" under the Grants No. DUT13LK01. M.G.R is partially supported by CONICET. We acknowledge the use of the CosmoMC and CAMB packages [36], [37]. We acknowledge the use of CCC for performing the statistical analysis.

[1] Y. Wang, Dark Energy (Wiley-vch Verlag GmbH and Co. KGaA, Berlin, 2010); Dark Energy: Observational and Theoretical Approaches, edited by Pilar Ruiz-Lapuente (Cambridge University Press, Cambridge, 2010).
[2] Nine-Year Wilkinson Microwave Anisotropy Probe (WMAP) Observations: Cosmological Parameter Results - WMAP Collaboration (Hins haw, G. et al.). Astrophys.J.Suppl. 208 (2013) 19 arXiv:1212.5226.
[3] Betoule M et al 2014 arXiv:1401.4064
[4] Planck 2013 results. I. Overview of products and scientific results - Planck Collaboration (Ade, P.A.R. et al.) arXiv:1303.5062.
[5] Planck 2013 results. XV. CMB power spectra and likelihood - Planck Collaboration (Ade, P.A.R. et al.) arXiv:1303.5075.
[6] Planck 2013 results. XVI. Cosmological parameters - Planck Collaboration (Ade, P.A.R. et al.) arXiv:1303.5076.
[7] Beutler, Florian et al. Mon.Not.Roy.Astron.Soc. 416 (2011) 3017-3032 arXiv:1106.3366 [astro-ph.CO]
[8] Padmanabhan, N., Xu, X., Eisenstein, D. J., Scalzo, R., Cuesta, A. J., Mehta, K. T., Kazin, E., arXiv:1202.0090
[9] Anderson, L., et al. 2012, arXiv:1203.6594.
[10] Blake, Chris et al. Mon.Not.Roy.Astron.Soc. 415 (2011) 2876 arXiv:1104.2948.
[11] Samushia, Lado et al. Mon.Not.Roy.Astron.Soc. 420 (2012) 2102-2119 arXiv:1102.1014; Samushia, Lado et al. Mon.Not.Roy.Astron.Soc. 429 (2013) 1514-1528 arXiv:1206.5309.
[12] E. Macaulay, I.K. Wehus, and H.K. Eriksen, Phys.Rev.Lett **111** 161301 (2013).
[13] Spyros Basilakos, [arXiv:1202.1637].
[14] Spyros Basilakos, Athina Pouri, [arXiv:1203.6724]; Athina Pouri, Spyros Basilakos, Manolis Plionis,[arXiv:1402.0964].
[15] Xu, Lixin Phys.Rev. D **87** (2013) 043525 arXiv:1302.2291; Xu, Lixin JCAP **1402** (2014) 048 arXiv:1312.4679.
[16] Xu, Lixin arXiv:1306.2683.
[17] Yang, Weiqiang et al. arXiv:1311.3419; Weiqiang Yang, Lixin Xu, Phys. Rev. D **89**, 083517 (2014); Weiqiang Yang, Lixin Xu, JCAP **08**(2014)034.
[18] Yang, Weiqiang et al. Phys.Rev. D **89** (2014) 043511 arXiv:1312.2769.
[19] Y. Wang, D. Wands, G.B. Zhao, L. Xu, arXiv:1404.5706; Yuting Wang, David Wands, Lixin Xu, Josue DeSantiago, Alireza Hojjati, Phys. Rev. D **87**, 083503 (2013); Lixin Xu, Yuting Wang, Hyerim Noh, Phys. Rev. D. **84**, 123004(2011).
[20] Amendola L., 2004, Phys. Rev., D **69**, 103524. L. Amendola, Phys. Rev. Lett. **86**, 196 (2001); L. Amendola and C. Quercellini, Phys. Rev. D **68**, 023514 (2003); L. Amendola, Phys. Rev. D **62**, 0043511 (2000).
[21] Zimdahl, Winfried et al. Phys.Lett. B **521** (2001) 133-138;Chimento, Luis P. et al. Phys.Rev. D **67** (2003) 083513.
[22] T. Koivisto, Phys. Rev. D **72**, 043516 (2005); H. Ziaeepour, Phys. Rev. D **86**, 043503 (2012).

[23] A. Pourtsidou, C. skordis, and E.J. Copeland, Phys. Rev. D **88**, 083505 (2013).

[24] Chimento, Luis P. et al. Phys.Rev. D**88** (2013) 087301; Chimento, Luis P. et al. Phys.Rev. D **85** (2012) 127301; Chimento, Luis P. et al. arXiv:1207.1492 [astro-ph.CO]; Chimento, Luis P. et al. Phys.Rev. D **84** (2011) 123507.

[25] E. Calabrese, D. Huterer, E. V. Linder, A. Melchiorri and L.Pagano, Phys.Rev.D **83** 123504 (2011).

[26] E. Calabrese, R. de Putter, D. Huterer, E. V. Linder, A. Melchiorri, Phys.Rev.D **83** 023011 (2011).

[27] Yun-He Li, Jing-Fei Zhang, Xin Zhang, arXiv:1404.5220.

[28] M.G. Richarte and L. Xu, arXiv:1407.0000.

[29] Valentina Salvatelli, Najla Said, Marco Bruni, Alessandro Melchiorri, and David Wands, arXiv: 1406.7297.

[30] W.Hu and I. Sawicki, Phys.Rev. D **76** (2007) 104043.

[31] W.Hu, Phys.Rev.D**77** 103524 (2008).

[32] Pedro G. Ferreira, Constantinos Skordis, Phys.Rev.D **81** 104020 (2010); Tessa Baker, Pedro G. Ferreira, Constantinos Skordis, Physical Review D **87**, 024015 (2013); C. Skordis, A. Pourtsidou, E. J. Copeland, arXiv:1502.07297.

[33] Valiviita, Jussi et al. JCAP **0807** (2008) 020, arXiv:0804.0232.

[34] Gavela, M.B. et al. JCAP **0907** (2009) 034, Erratum-ibid. 1005 (2010), arXiv:0901.1611.

[35] Jackson, Brendan M. et al. Phys.Rev. D **79** (2009) 043526, arXiv:0901.3272; Majerotto, Elisabetta et al. Mon.Not.Roy.Astron.Soc. **402** (2010) 2344-2354, arXiv:0907.4981; Valiviita, Jussi et al. Mon.Not.Roy.Astron.Soc. **402** (2010) 2355-2368, arXiv:0907.4987; Clemson, Timothy et al. Phys.Rev. D **85** (2012) 043007, arXiv:1109.6234.

[36] Lewis, Antony et al. Phys.Rev. D**66** (2002) 103511. astro-ph/0205436, http://cosmologist.info/cosmomc/.

[37] Lewis, Antony et al. Astrophys.J. **538** (2000) 473-476. astro-ph/9911177, http://camb.info/.

[38] L.P.Chimento, Phys.Rev.D **81** 043525 (2010).

[39] H. Kodama and M. Sasaki. 1984. Prog.Theor.Phys.,**78**,1.

[40] Ma, Chung-Pei et al. Astrophys.J. **455** (1995) 7-25 astro-ph/9506072.

[41] Clemson, Timothy et al. Phys.Rev. D 85 (2012) 043007, arXiv:1109.6234.

[42] Koyama K., Maartens R., Song Y.-S., 2009, JCAP, **0910**, 017.

[43] W. Yang and L. Xu, 1401.5177.

[44] Weiqiang Yang, Lixin Xu, Phys. Rev. D **90**, 083532 (2014), arXiv:1409.5533.

[45] Planck 2015 results. XIII. Cosmological parameters, P. A. R. Ade et al. arXiv:1502.01589.